Biochimica et Biophysica Acta 1848 (2015) 615–621

Contents lists available at ScienceDirect

Biochimica et Biophysica Acta

journal homepage: www.elsevier.com/locate/bbamem

Differential repositioning of the second transmembrane helices from *E. coli* Tar and EnvZ upon moving the flanking aromatic residues

Salomé C. Botelho [a,1], Karl Enquist [a,2], Gunnar von Heijne [a], Roger R. Draheim [b,c,*]

[a] Department of Biochemistry and Biophysics, Stockholm University, Svante Arrhenius väg 16C, SE-10691 Stockholm, Sweden
[b] Division of Pharmacy, Durham University, Queen's Campus, Stockton-on-Tees TS17 6BH, England, UK
[c] Wolfson Research Institute for Health and Wellbeing, Durham University, Queen's Campus, Stockton-on-Tees, TS17 6BH, England, UK

ARTICLE INFO

Article history:
Received 9 July 2014
Received in revised form 29 October 2014
Accepted 17 November 2014
Available online 21 November 2014

Keywords:
Aromatic tuning
Hydrophobic-polar membrane interface
Interfacial anchoring
Transmembrane helices
Glycosylation mapping

ABSTRACT

Aromatic tuning, i.e. repositioning aromatic residues found at the cytoplasmic end of transmembrane (TM) domains within bacterial receptors, has been previously shown to modulate signal output from the aspartate chemoreceptor (Tar) and the major osmosensor EnvZ of *Escherichia coli*. In the case of Tar, changes in signal output consistent with the vertical position of the native Trp-Tyr aromatic tandem within TM2 were observed. In contrast, within EnvZ, where a Trp-Leu-Phe aromatic triplet was repositioned, the surface that the triplet resided upon was the major determinant governing signal output. However, these studies failed to determine whether moving the aromatic residues was sufficient to physically reposition the TM helix within a membrane. Recent coarse-grained molecular dynamics (CG-MD) simulations predicted displacement of Tar TM2 upon moving the aromatic residues at the cytoplasmic end of the helix. Here, we demonstrate that repositioning the Trp-Tyr tandem within Tar TM2 displaces the C-terminal boundary of the helix relative to the membrane. In a similar analysis of EnvZ, an abrupt initial displacement of TM2 was observed but no subsequent movement was seen, suggesting that the vertical position of TM2 is not governed by the location of the Trp-Leu-Phe triplet. Our results also provide another set of experimental data, i.e. the resistance of EnvZ TM2 to being displaced upon aromatic tuning, which could be useful for subsequent refinement of the initial CG-MD simulations. Finally, we discuss the limitations of these methodologies, how moving flanking aromatic residues might impact steady-state signal output and the potential to employ aromatic tuning in other bacterial membrane-spanning receptors.

Published by Elsevier B.V.

1. Introduction

Two-component signaling circuits allow bacteria to detect and respond to external stimuli. However, for the majority of these circuits, the input stimulus remains unidentified. To circumvent this limitation, we developed an "aromatic tuning" technique, i.e. repositioning the aromatic residues commonly found at the cytoplasmic end of the transmembrane domain of receptors within these circuits, to modulate steady-state signal output from the aspartate chemoreceptor (Tar) and EnvZ, a major osmosensor, from *Escherichia coli* [1,2]. In essence, aromatic tuning allows stimulus-independent modulation of bacterial signaling circuits, which can be used to control particular physiological or developmental processes without determination of the input stimulus. Aromatic residues are conserved in similar locations in other receptors, suggesting that our tuning approach could be applied to a wide variety of other two-component signaling circuits [3,4].

Aromatic tuning was initially inspired by studies with α-helical peptides that possess an aliphatic core of Ala-Leu repeats flanked by Trp (WALP) or Tyr (YALP) residues. These Trp and Tyr residues demonstrated a distinct preference for the polar/hydrophobic interfaces between the headgroups and acyl chains of synthetic lipid bilayers [5,6]. Furthermore, a glycosylation-mapping technique [7] highlighted the ability of Trp and Phe residues to reposition poly-Leu TM helices in membranes due to their affinity for polar/hydrophobic interfaces [8]. Other studies have compared the biophysical effects of having single or tandem aromatic residues at the end of these poly-Ala-Leu α-helical peptides with respect to their preferred orientation and dynamics within different synthetic

Abbreviations: WALP or YALP, α-helical peptides that possess an aliphatic core of Ala-Leu repeats flanked by Trp (WALP) or Tyr (YALP) residues; TM, transmembrane; TM2, second transmembrane helix; SHK, sensor histidine kinase; CG-MD, coarse-grained molecular dynamics; MGD, minimum glycosylation distance; AS1, amphipathic sequence 1; AS2, amphipathic sequence 2; RM, rough microsomes

* Corresponding author at: Durham University, Division of Pharmacy, Wolfson Building, Room F106, Stockton-on-Tees TS17 6BH, England, UK. Tel.: +44 191 334 0694; fax: +44 191 334 03740.
E-mail address: roger.draheim@durham.ac.uk (R.R. Draheim).
[1] Current addresses: Department of Molecular and Cellular Physiology, Howard Hughes Medical Institute, Lorry Lokey SIM1 Building 07-535, 265 Campus Drive Room G1021, Stanford University School of Medicine, Stanford, CA, 94305-5453, United States of America.
[2] Current addresses: OrganoClick AB, Ritarslingan 20, SE-18766, Täby, Sweden.

http://dx.doi.org/10.1016/j.bbamem.2014.11.017
0005-2736/Published by Elsevier B.V.

bilayers [9,10]. Therefore, substantial biochemical and biophysical evidence suggested that repositioning the aromatic residues at the end of the TM2 helices would dramatically affect the properties of these signaling helices and likely modulate signal output from membrane-spanning receptors in which they were moved.

When we initially attempted aromatic tuning, the mechanistic models for transmembrane signaling by Tar were based on piston-type displacements of TM2 [1,4,11–14]. We originally hypothesized that aromatic tuning would displace TM2 of Tar within the membrane [1]. To examine this hypothesis, a series of Tar receptors was created where the Trp-Tyr tandem found at the cytoplasmic end of TM2 was moved up to three residue steps in either direction (Fig. 1A). It is important to note that Tar is not a canonical sensor histidine kinase (SHK), requires CheW and CheA to form functional intracellular signaling complexes, and controls the direction of flagellar rotation rather than gene transcription (Fig. 1B) [15–18]. When these Tar receptors were expressed within intact *E. coli* cells, an increase in steady-state signal output was observed that was consistent with the vertical position of the aromatic residues within TM2 (Fig. 1C) [1].

In order to determine whether aromatic tuning would work within a canonical SHK, we examined its effectiveness using the major *E. coli* osmosensor, EnvZ, where a rotation of TM2 has been proposed as the mechanism of transmembrane communication [19–23]. More recently, regulated unfolding [24] and scissor-like models have been proposed for signaling by SHKs [25,26]. Due to this variety of proposed mechanisms, we were unsure of what pattern of signal outputs would be observed upon aromatic tuning. Within EnvZ, a Trp-Leu-Phe triplet was repositioned and an anti-symmetrical fluorescent reporter system was employed to monitor steady-state signal output. In this case, we observed that the surface of TM2 that the aromatic residues reside upon was the major determinant in signal output rather than their vertical position (Fig. 1D and E) [2].

In our previous studies, we did not directly demonstrate that moving the aromatic residues within TM2 of Tar or EnvZ was sufficient to reposition either helix relative to the cytoplasmic membrane [1,2]. However, recent coarse-grained molecular dynamics (CG-MD) simulations support the displacement of Tar TM2 when aromatic tuning is employed [27]. Here, we utilize a glycosylation-mapping technique to determine

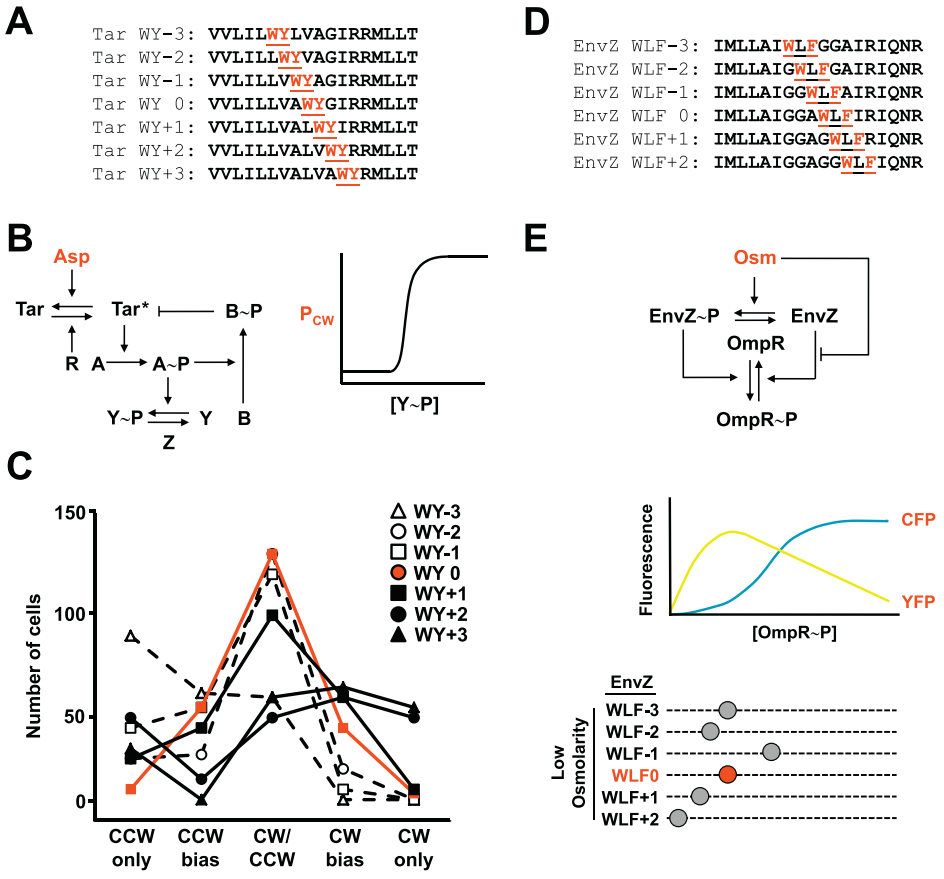

Fig. 1. Synopsis of results from aromatic tuning of Tar and EnvZ TM2. (A) Within Tar TM2, a Trp-Tyr (red) was moved about its original position at the cytoplasmic polar/hydrophobic interface [1]. (B) The chemotactic circuit of *E. coli* [53]. Chemotaxis proteins are denoted by a single letter, e.g. CheR denoted as "R", and the activated form of Tar is indicated with an asterisk (Tar*). Aspartate (Asp) binds to Tar and promotes the inactive form, which results in decreased intracellular levels of CheY-P. The intracellular level of CheY-P governs the probability of clockwise flagellar rotation (P_{CW}) [54]. (C) Rotation of a single flagellum from roughly 200 independent cells expressing one of the aromatically tuned variants was analyzed for 30 s and classified into one of five categories (left to right): rotating exclusively CCW, rotating mostly CCW with occasional reversals, rapidly switching between both rotational directions (CW/CCW), rotating mostly CW with occasional reversals and rotating exclusively CW. As P_{CW} increases, the number of cells in each category shifts from the left end of the axis toward the right end. In summary, the lowest overall P_{CW} was observed from cells expressing the WY-3 variant, while the greatest was observed from cells expressing the WY + 2 or WY + 3 variants. In the case of Tar, the vertical position of the aromatic residues correlates with P_{CW} [1]. (D) When aromatic tuning was performed in EnvZ, a Trp-Leu-Phe triplet (red) was repositioned [2]. (E) The EnvZ/OmpR osmosensing circuit of *E. coli*. EnvZ is a bifunctional SHK that phosphorylates and dephosphoryates its cognate RR, OmpR. Osmotic pressure (Osm), depicted in red, due to the presence of small inner membrane-impermeable solutes, alters the ratio of these activities resulting in a net increase of intracellular OmpR-P. The intracellular level of OmpR-P governs transcription of *ompF* (yellow) and *ompC* (blue) and was monitored by employing an *E. coli* strain that contains a transcriptional fusion of *yfp* to *ompF* and of *cfp* to *ompC*. Intracellular levels of OmpR-P were estimated by calculating the CFP/YFP ratio (red). The gray-filled circles on the dashed lines indicate the estimated OmpR-P levels in cells expressing one of the aromatically tuned variants at intermediate levels. Aromatic tuning in EnvZ resulted in a pattern of signal output that did not correlate with the vertical position of the aromatic residues but appeared more helical in distribution suggesting that the surface of TM2 that the residues were located upon was of greater importance [2].

whether repositioning the aromatic residues is sufficient to displace the membrane-embedded TM2 helices from Tar and EnvZ [7]. We demonstrate that repositioning the aromatic residues, a Trp-Tyr tandem, that normally reside at the cytoplasmic end of Tar TM2 resulted in a series of small incremental changes in minimal glycosylation distance (MGD) consistent with repositioning the C-terminal boundary of the helix. In the case of EnvZ, a Trp-Leu-Phe triplet was repositioned, and after an abrupt initial displacement, no further substantial displacements were observed. We propose that this large initial displacement is likely due to a loss of interaction between an arginyl residue and the membrane, and that a pattern consistent with increasing TM2 displacement due to aromatic tuning was not observed. We conclude by suggesting that differences observed between the behavior of helices are due to the inherently different properties of the residues being repositioned (i.e. Trp or Tyr versus Phe). We also discuss the limitations of these methodologies, how moving flanking aromatic residues might impact steady-state signal output and the potential to employ aromatic tuning in other bacterial membrane-spanning receptors.

2. Materials and methods

2.1. Selection of residues comprising TM2 of Tar and EnvZ

The primary sequences of Tar (GI: 16129838) and EnvZ (GI: 16131281) from *E. coli* K-12 MG1655 were subjected to a full protein scan with the ΔG predictor using a minimal window of 9 residues and a maximal window of 40 residues [28]. This software searches the protein sequences for putative TM helices by employing a sliding window of variable lengths and calculating the ΔG_{app} for transmembrane insertion throughout the length of the sequence. In the case of Tar, residues between Tyr-187 and Leu-217 were predicted to comprise TM2, while Leu-160 to Ile-181 were proposed for EnvZ. In both cases, a motif commonly found within transmembrane helices that consisted of positively charged residues and adjacent aromatic resides bracketing a core of aliphatic residues was found within the predicted TM segments [29]. Based on this observation, Arg-188 to Arg-213 from Tar and Arg-162 to Arg-180 from EnvZ were selected for glycosylation-mapping analysis.

2.2. Glycosylation-mapping analysis

Model Lep proteins including the TM2 segments from Tar and EnvZ were expressed in vitro from plasmid pGEM1 (Stratagene). To create the initial model Lep protein, the 5′ end of the *lepB* gene from *E. coli* was modified by the introduction of an *Xba*I site and by changing the sequence 5′ to the initiator ATG codon to a Kozak consensus sequence [30]. These proteins contained one acceptor site for N-linked glycosylation in positions 3–5 (Asn-Ser-Thr; G1 in Fig. 2A) included within an extended sequence of 24 residues (Met-Ala-Asn^3-Ser-Thr-Ser-Gln-Gly-Ser-Gln-Pro-Ile-Asn-Ala-Gln-Ala-Ala-Pro-Val-Ala-Gln-Gly-Gly-Ser-Gln-Gly-Glu-Phe^5) inserted between Asn^3 and Phe^5 in the wild-type sequence of Lep. A series of proteins that contained a second acceptor site (Asn-Ser-Thr; G2 in Fig. 2A) placed at single-residue increments between positions 87–90 (d = 6 construct) and positions 92–94 (d = 11 construct) were created using standard site-directed mutagenesis techniques (Stratagene). The predicted TM2 helices from either Tar or EnvZ were introduced between an *Spe*I site in codons 60–61 and a *Kpn*I site in codon 80 of the *lepB* gene using standard PCR amplification methods [31]. Plasmids pRD200 [4] or pEnvZ [32] served as templates for Tar or EnvZ, respectively. The oligonucelotides used during the amplification introduced a flanking tetraresidyl sequence (Gly-Pro-Gly-Gly) to reduce the propensity for the formation of secondary structure that could alter the distance between the second accepting site (G2) and the active site of OST [33]. Other Lep proteins were made by moving the residues within TM2 of Tar (Trp-Tyr) or EnvZ (Trp-Leu-Phe) using standard site-directed mutagenesis techniques (Stratagene) (Figs. 3A and 4A).

2.3. Expression in vitro and quantification of glycosylation

The Lep proteins cloned in pGEM1 were transcribed and translated in vitro using the TNT Quick Coupled Transcription/Translation System

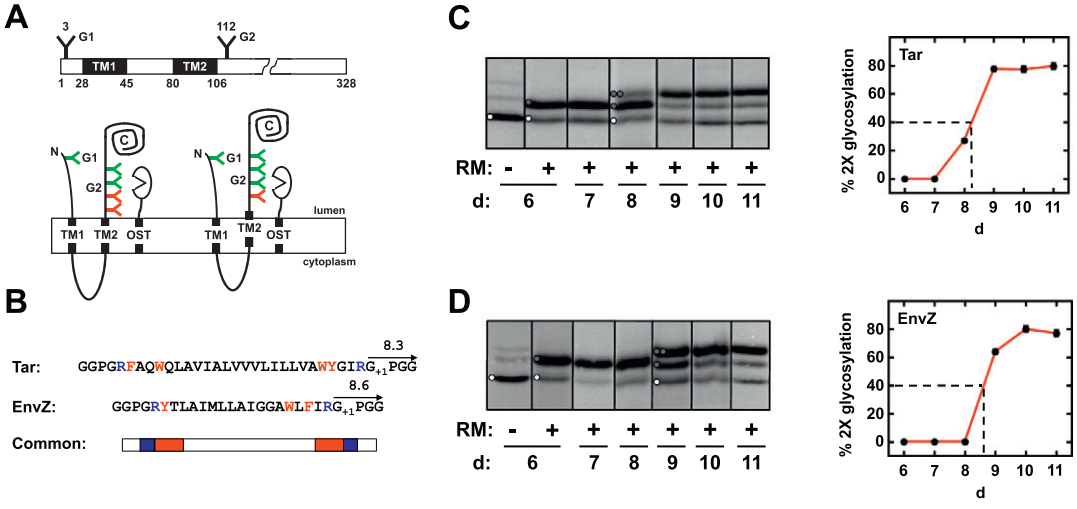

Fig. 2. Minimum glycosylation distance (MGD) analysis of Tar and EnvZ TM2. (A) Linear and topological characteristics of the model Lep protein used in this study. The model protein contains a glycosylation-accepting site (G1) more than 20 residues away from the lumenal boundary TM1 and a second glycosylation-accepting site (G2) that is positioned between 6 and 11 residues (d = 6 to d = 11) from the boundary of TM2. If TM2 is displaced, the position of the second G2 relative to the boundary of the membrane will change and allow a previously unglycosylated accepting site (red) to become glycosylated (green). It is also possible to monitor displacements of TM2 into the membrane. (B) Primary sequence of TM2s used for glycosylation-mapping analysis. A motif commonly found in transmembrane helices consisting of flanking positively charged residues (blue), adjacent aromatic residues (red) and an aliphatic core (uncolored) was present in both segments. The flanking Gly-Pro-Gly-Gly tetrapeptide was included to reduce the propensity for formation of secondary structure. The first Gly of the flanking tetrapeptide (G_{+1}) is considered the first residue (d = 1) outside of TM2. MGD values for each segment are provided above the primary sequence. (C) Identification and analysis of the different species by SDS-PAGE. The presence of rough microsomes (RM) facilitates glycosylation due to the presence of oligosaccharyltransferase (OST). Differences in migration allow identification of the unglycosylated (single white dot), singly glycosylated (G1 only; single gray dot) and the doubly glycosylated moieties (G1 and G2; two gray dots). An increase in the doubly glycosylated moiety is observed as G2 is moved further away from the boundary of TM2 from Tar. MGD is calculated as the number of residues (d) required to achieve 40% double glycosylation (dashed line). The MGD for Tar TM2 was found to be 8.3. (D) A similar analysis was performed with EnvZ TM2 and a value of 8.6 was determined for the MGD (dashed line).

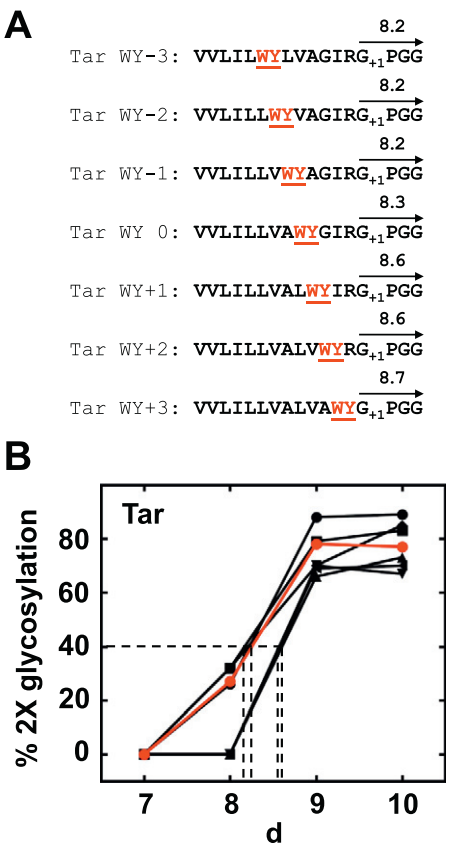

Fig. 3. Glycosylation-mapping analysis of aromatically tuned Tar TM2 segments. (A) Primary sequence of the C-terminal end of Tar TM2. Within the segment, a Trp-Tyr tandem was moved (red). MGD values are provided above the primary sequence of each segment. (B) As described in Fig. 2C, the amount of the doubly glycosylated moiety correlates with the number of residues between the end of TM2 and G2. Results are provided for the modified TM2 segments from Tar: −3 variants as filled circles; −2 variants as filled squares; −1 variants as filled diamonds; +1 variants as filled downward-pointing triangles; +2 variants as filled upward-pointing triangles; and +3 variants as filled leftward-pointing triangles. The red line indicates results for receptors containing the aromatic residues at their original position. MGDs were determined via the dashed lines.

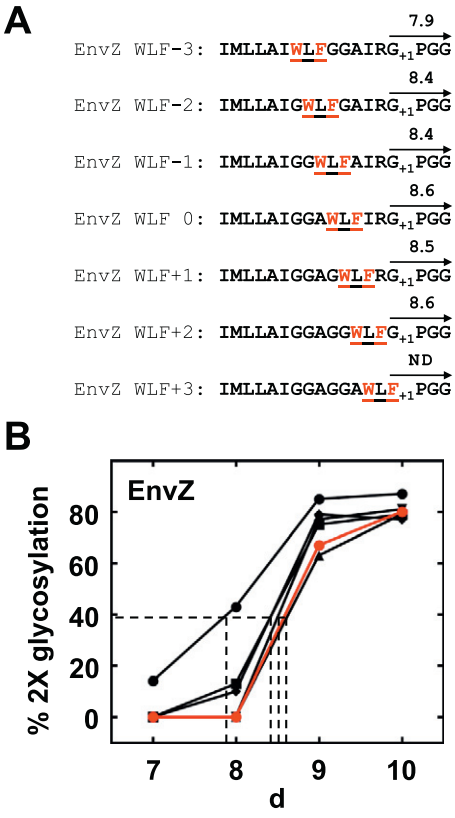

Fig. 4. Glycosylation-mapping analysis of aromatically tuned EnvZ TM2 segments. (A) Primary sequence of the C-terminal end of EnvZ TM2. Within the segment, a Trp-Leu-Phe triplet was moved (red). MGD values are provided above the primary sequence of each segment. ND indicates that the MGD was not determined. (B) As described in Fig. 2C, the amount of the doubly glycosylated moiety correlates with the number of residues between the end of TM2 and G2. Results are provided for the modified TM2 segments from EnvZ: −3 variants as filled circles; −2 variants as filled squares; −1 variants as filled diamonds; +1 variants as filled downward-pointing triangles; and +2 variants as filled upward-pointing triangles. The red line indicates results for the receptor containing the aromatic residues at their original position. MGDs were calculated via the dashed lines.

(Promega) as previously described [34]. Briefly, 1 μg of DNA template, 1 μL of ^{35}S-Met (5 μCi), and 0.5 μL of dog pancreas rough microsomes were added at the start of the reaction, and samples were incubated for 90 min at 30 °C. To stop the reaction, 40 μL of SDS sample buffer was added and the samples were incubated at 95 °C for 5 min, centrifuged for 2 min in a table-top microfuge (13,000 ×g) and 6 μL was loaded on a 10% SDS/polyacrylamide gel. Translation products were analyzed by SDS-PAGE, and gels were analyzed on a Fuji FLA-3000 PhosphorImager with the Image Reader v1.8J and Image Gauge v4.22 software (Fujifilm). The extent of glycosylation was quantified with QtiPlot v0.9.7.5. To calculate the percentage of doubly glycosylated (% 2× glycosylated), the quotient of the intensity of the doubly glycosylated band to the summed intensities of the singly and doubly glycosylated bands was calculated. The unglycosylated molecules that have not been targeted to the microsomes are ignored but, in general, represent less than 25% of the total Lep present. In most cases, the glycosylation efficiency varied by no more than 3% between different experiments.

3. Results

3.1. Overview of glycosylation-mapping analysis

Glycosylation-mapping analysis [7] was used to monitor changes in the position of TM2 segments within the membrane. This technique is based upon the ability of the luminally located endoplasmic reticulum enzyme oligosaccharyl transferase (OST) to add a glycan to the Asn residue in Asn-Xaa-(Ser/Thr) glycosylation acceptor sites within target proteins. The Lep model protein we used contains an N-terminal acceptor site for *N*-linked glycosylation (G1) to ensure that the analysis includes only protein that becomes embedded within the microsomal membrane used in the assay (Fig. 2A). It also contains a second acceptor site (G2) that is incrementally moved further away from the lumenal face of the microsomal membrane. This movement allows the active site of OST to act as a molecular ruler because each acceptor site will be glycosylated to an extent that correlates with the distance between the active site of OST and the acceptor site (G2). In Fig. 2A, the red acceptor sites are not far enough from the lumenal membrane to become glycosylated, whereas the green sites are distal enough to become glycosylated. This technique was previously used to measure the N- and C-terminal boundaries of several human α and β integrin subunits [35,36]. The subsequent high-resolution structures of the transmembrane domains of αIIb monomer [37], the β3 monomer [38] and the αIIbβ3 heterodimer [39] confirmed these boundaries thereby lending credence to glycosylation-mapping analysis. In addition, similar changes in the pattern of glycosylation have been previously observed due to moving aromatic residues throughout the C-terminal half of a poly-Leu transmembrane segment [8] suggesting that the technique is adequate for detecting TM segment repositioning due to aromatic tuning.

3.2. Baseline positions of TM2 from Tar and EnvZ

Based on the previous success with determining TM boundaries by glycosylation mapping, we performed similar studies with TM2 from Tar and EnvZ (Fig. 2B). It should be noted that the segments of interest are also flanked by two tetrapeptide sequences (Gly-Gly-Pro-Gly…Gly-Pro-Gly-Gly) that serve to break secondary structure that could adversely affect comparisons between different segments (Fig. 2B). The Gly residue denoted with a +1 subscript in Fig. 2B was considered as the first non-transmembrane residue. The percentage of unglycosylated, singly glycosylated, and doubly glycosylated protein can be readily determined by SDS-PAGE because the glycosylated forms of the protein migrate less rapidly (Fig. 2C). We began by analyzing the TM2 segment of Tar, and no glycosylation of G2 was observed when six (d = 6) or seven (d = 7) residues were present between the boundary of the TM2 segment and G2. Moving G2 an additional residue-step away from the membrane (d = 8) resulted in approximately 30% of the embedded Lep protein undergoing two glycosylation events. Further movement of G2 away from the lumenal surface (d ≥ 9) resulted in about 80% of total embedded protein becoming doubly glycosylated, which approximates the maximal extent previously observed under these experimental conditions (Fig. 2C) [7]. To quantitatively compare TM segment position, the minimal glycosylation distance (MGD), i.e., the number of residues required for half-maximal glycosylation (defined as the value of d for which glycosylation efficiency is 40%), was calculated. For Tar TM2, the MGD was determined to be 8.3 (Fig. 2C).

The series of Lep proteins containing EnvZ TM2 exhibited no glycosylation of G2 when d = 6, 7 or 8. Repositioning G2 another residue away from the lumenal surface resulted in about 60% of the embedded Lep protein becoming doubly glycosylated. Moving the accepting site an additional residue (d = 10) resulted in the previously observed maximal value of approximately 80% of the embedded protein becoming doubly glycosylated [7]. For EnvZ TM2, the MGD was determined to be 8.6 (Fig. 2D). This increase in MGD indicates that more residues are required C-terminal to the EnvZ TM2 segment in order to appropriately position the G2 acceptor site for glycosylation by OST.

3.3. TM2 of Tar is increasingly repositioned upon moving the Trp-Tyr tandem

To monitor possible helix-repositioning effects due to aromatic tuning, a series of Lep proteins containing segments in which the Trp-Tyr tandem was moved up to three residues toward (minus-series) or away from (plus-series) the center of Tar TM2 were created (Fig. 3A). Subsequently, this series of Lep proteins was used as a template to create additional subsets that contained a G2 acceptor site in single-residue increments from seven (d = 7) to ten (d = 10) residues away from the lumenal end of TM2. The creation of this library of Lep proteins allowed the glycosylation-mapping assay described in Fig. 2 to be performed on each tuned TM2 segment from Tar (Fig. 3A). Analysis of these aromatically tuned Tar segments resulted in trends similar to the un-tuned version (Fig. 2C). For each segment, the minimal extent of G2 glycosylation was observed at d = 7 and the maximal extent at d = 10 (Fig. 3B). During parallel analysis of the aromatically tuned Tar variants, an MGD of 8.2 was observed for WY-3 through WY-1 segments compared to the wild-type segment (WY 0) that possessed an MGD of 8.3. The WY + 1 and WY + 2 segments possessed MGDs of 8.6, while the WY + 3 segment had an MGD of 8.7 (Fig. 3B). We previously demonstrated that employing aromatic tuning at the C-terminus of TM2 of Tar resulted in incremental changes in steady-state signal output (Fig. 1C) [1]. These glycosylation-mapping results are consistent with repositioning of the cytoplasmic boundary of Tar TM2 during aromatic tuning. However, other options such as a partial unwinding of the helix cannot be ruled out with this methodology.

3.4. TM2 of EnvZ remains more stationary upon moving the Trp-Leu-Phe triplet

In a similar manner, a series of Lep proteins containing segments in which the Trp-Leu-Phe triplet within EnvZ was moved up to three residues toward (minus-series) or away from (plus-series) the center of TM2 were created. These were subsequently used as templates to create additional subsets that contained a G2 acceptor site in single-residue increments from seven (d = 7) to ten (d = 10) residues away from the lumenal end of TM2 (Fig. 4A). The MGD values demonstrate that the C-terminus of the WLF-3 segment was displaced out of the membrane (MGD = 7.9), while the other segments possessed MGDs ranging from 8.4 to 8.6 (Fig. 4B). Analysis of the EnvZ WLF + 3 segment resulted in the accumulation of a lower molecular weight product consistent with cleavage of TM2 (presumably by the signal peptidase) from the Lep model protein [34]. Based on this result, we did not analyze the segment any further. In the case of most EnvZ segments, changes in MGD are small and not steadily increasing when compared to changes observed with Tar, which suggests that an incremental repositioning of EnvZ TM2 does not occur. We suspect that this abrupt transition is due to the Trp-Leu-Phe triplet repositioning the C-terminal boundary to such an extent that the basic guanido group from the Arg side-chain can no longer interact with the acidic phospholipid head groups (Fig. 5). Arginyl side-chains have been shown to snorkel five to six residues along a transmembrane helix [40] and it is possible that the WLF-3 segment is displaced to such an extent that the Arg side-chain cannot contribute to the positioning of the C-terminus [41].

4. Discussion

4.1. Differences in the initial position of TM2 helices and their subsequent repositioning

We have measured the minimum glycosylation distance (MGD) of TM2 segments from Tar and EnvZ and observed that the segment from EnvZ is embedded slightly deeper into the membrane than the counterpart from Tar, as observed by MGDs of 8.6 and 8.3, respectively. These results are consistent with a previous study that demonstrated an inverse correlation between the length of a poly-Leu TM segment and its relative MGD [7]. However, the difference in MGD for the TM2 segments (~0.3) is less than what would be expected for poly-Leu TM segments of similar lengths (~1.5). This suggests that the affinity of the amphipathic aromatic residues (Trp and Tyr) for the membrane interfacial region [5,6,8], the preference of Phe residues for the aliphatic membrane core [8] and the interactions of the positively charged Arg residues with the negative phosopholipids [41] are also relevant in the positioning of the TM2 segments within the membrane.

A previous study that employed comparative CG-MD simulations to examine the ability of aromatic tuning to displace Tar TM2 in the presence of an explicit membrane and solvent demonstrated that moving the Trp-Tyr residue was sufficient to induce small TM2 displacements of up to 1.5 Å [27]. Assuming that the region in Lep that contains the G2 glycosylation site is in an extended conformation, a shift in MGD of 0.5 residues as seen for the Tar constructs corresponds to a shift in the positioning of the TM2 helix of 1.6–1.7 Å, close to the CG-MD results. It should also be noted that the median value of the ensemble from all simulations is in agreement with our MGD values for the aromatically tuned Tar TM2 helices. In both the CG-MD simulations and MGD analysis, similar patterns of displacement were observed, i.e. a grouping of the minus-series of receptors with similar displacements toward the cytoplasm (WY-3 through WY-1), a baseline position for the wild-type (WY 0), two receptors that are slightly displaced toward the periplasm (WY + 1 and WY + 2) and a larger shift toward the periplasm for the WY + 3 variant (Fig. 3). We propose that the absence of EnvZ TM2 displacement should be comparatively assessed by CG-MD simulation. In the case of EnvZ, moving the Trp-Leu-Phe triplet did not generate

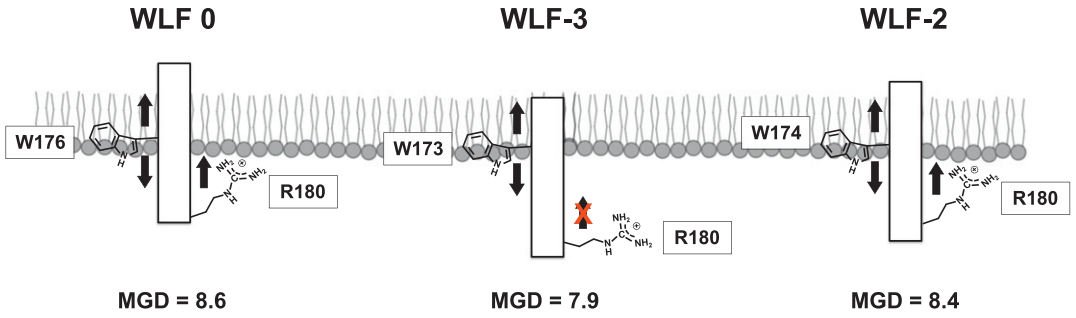

Fig. 5. Proposed model for the large difference in MGD values for the WLF-3 and WLF-2 variants of EnvZ. We propose that the baseline position of EnvZ TM2 (WLF 0) is due to both the interaction of Trp-176 with the polar/hydrophobic interfacial region and due to snorkeling of the Arg-180 side chain to interact with the negatively charged phospholipids (left). One possibility for the large change in MGD observed between WLF-3 (7.9) and WLF-2 (8.4) is that upon moving the Trp into the membrane at residue position 173, TM2 is displaced out of the membrane to such an extent that the Arg residue at residue position 180 can no longer snorkel and interact with the negatively charged lipids (center). When the Trp residue is moved one more step toward the interface, i.e. at position 174, the side chain or the Arg residue is in a position where it could still interact with the membrane surface (right).

large changes in MGD, with the exception of the WLF-3 variant, which could be due to the fact that the helix displaced to such an extent that the Arg side-chain cannot contribute to the positioning of the C-terminus [41].

4.2. Limitations of an optimized single-helix approach during analysis of transmembrane communication

It is important to note that the context of TM2 within the full-length Tar and EnvZ receptors is likely more complex than single independently acting α-helices. For example, within the CG-MD simulations described above, contiguous optimized α-helices are explicitly forced [27]. Likewise, within the glycosylation-mapping assay, the flanking tetrapeptide (Gly-Gly-Pro-Gly … Gly-Pro-Gly-Gly) is employed as a helix-breaker to ensure that all residues downstream are in an extended form, however, the ability to prevent the membrane-embedded TM helix from partially unwinding has not been probed [33]. Thus, when small fractional differences in MGD are observed, a partial unwinding of the transmembrane helix cannot be explicitly ruled out.

Recently, a vast amount of structural, biochemical and genetic information has been integrated into a "regulated unfolding" model of intraprotein signaling by SHKs [24]. This model proposes that modular proteins are composed of individually folding domains that contribute distinct functionalities to overall protein function. Within SHKs, the effector domain has been suggested to be maintained in an inactive conformation by a rigid connection between the stimulus perception and effector domains. Upon perception of stimulus, this structurally labile connection would be disengaged in a manner that would allow the effector domain to adopt an active conformation [24]. Previous biophysical analyses have demonstrated that the presence of tandem amphipathic aromatic residues, Trp or Tyr, at one end of a transmembrane α-helix promotes increased conformational dynamics compared to the presence of a single Trp or Tyr. This increase has been proposed to be based upon the ability of the Trp and Tyr residues to form hydrogen bonds with the polar head groups and interfacial water molecules. Consistent with these expectations, the presence of two Phe residues is not remarkably different from a single Trp, Tyr or Phe residue [9,10].

One intriguing possibility is that increased conformational dynamics at the cytoplasmic end of TM2 could facilitate partial unwinding of the TM helix. Within intact bacterial membrane-spanning receptors, the region connecting the TM to the HAMP domain is colloquially referred to as a "control cable" because its residue composition governs coupling of signal transduction between adjacent domains [1,4,42–49]. As proposed by the dynamic bundle of HAMP signal transmission, this partial unwinding of the cytoplasmic end of TM2 could lead to destabilization of AS1, the N-terminal helix within the HAMP domain, and thus to changes in AS2 and AS2′ that could subsequently be transmitted downstream to the domains responsible for signal output [42–44,49]. Alternatively, within the context of the gearbox model, it is possible that a destabilization of AS1 would lead to interconversion from knobs-to-knobs packing into a more canonical knobs-into-holes packing and thus leading to downstream signaling [19–23]. Therefore, we hypothesize that the Trp-209/Tyr-210 tandem in *E. coli* Tar maintains the baseline level of conformational dynamics at the cytoplasmic end of TM2, such that a piston-type displacement of TM2 enhances interactions of the aromatic tandem with the polar headgroups and interfacial waters to a degree that promotes "regulated unfolding" of the membrane-adjacent HAMP domain. In the case of EnvZ, moving the Trp-Leu-Phe, while clearly central to the concept of aromatic tuning, may not modulate dynamics at the cytoplasmic end of TM2, as only a single amphipathic aromatic residue (Trp) exists in conjunction with a largely hydrophobic residue (Phe) [9,10].

From another slightly different, albeit interesting perspective, Trp-containing regions in certain helical orientations have been shown to promote dimerization of Tar TM domains [50]. Therefore, moving the Trp residues may alter helix packing within Tar and EnvZ TM domains and thus facilitate changes in the overall dynamic stability of the cytoplasmic end of the TM bundle. Lending support to this concept is a study proposing that the presence of a water-filled hemi-channel within the cytoplasmic end of the TM bundle is a critical component of signal transduction within *E. coli* PhoQ [51]. It is possible that moving the aromatic residues around the surface of TM2 results in certain positions where the aromatic residues would be positioned into this water-filled hemi-channel, which could ultimately result in changes to PhoQ baseline signal output. Therefore, it remains important to apply the optimized single-helix results presented here to the greater complexities of transmembrane communication within the context of a full-length membrane-spanning receptor.

4.3. Wider adoption of aromatic tuning

In our previous studies, we demonstrate that aromatic tuning results in changes in signal output from both Tar and EnvZ, however, a difference in the pattern of signal outputs was observed (Fig. 1) [1,2]. This pattern of signal outputs shows that even though aromatic tuning did not displace the TM2 helix of EnvZ (Fig. 4), it was still effective in modulating signal output within the full-length receptor. In that regard, we suggest that aromatic tuning was able to achieve its initial goal of stimulus-independent modulation of a two-component signaling circuit. Published sequence alignments have shown that aromatic residues are often found at the cytoplasmic end of the final transmembrane helix within bacterial membrane-spanning receptors [3,4] suggesting that aromatic tuning will be useful for research groups working with other two-component circuits. We hope that these results, in conjunction with our previous demonstration of the differences in α-helicity of AS1 segments [52], promote continued discussion about the

mechanisms of transmembrane communication within bacterial membrane-spanning receptors.

Acknowledgments

Members of the von Heijne group provided valuable support and discussion during the early stages of the manuscript. S. C. B. was supported by a graduate student fellowship (SFRH/BD/26017/2007) from Fundação para a Ciência e a Tecnologia, Portugal. This work was also supported by grants from the Swedish Foundation for Strategic Research, the Swedish Research Council and the Swedish Cancer Foundation to G. v. H. A Kirschstein National Research Service Award from the National Institutes of Health (AI075573) supported R. R. D. during the initial phases of this work.

References

[1] R.R. Draheim, A.F. Bormans, R.Z. Lai, M.D. Manson, Tuning a bacterial chemoreceptor with protein–membrane interactions, Biochemistry 45 (2006) 14655–14664.
[2] M.H. Norholm, G. von Heijne, R.R. Draheim, 'Forcing the issue' — aromatic tuning facilitates stimulus-independent modulation of a two-component signaling circuit, ACS Synth. Biol. (2014), http://dx.doi.org/10.1021/sb500261t.
[3] T. Boldog, G.L. Hazelbauer, Accessibility of introduced cysteines in chemoreceptor transmembrane helices reveals boundaries interior to bracketing charged residues, Protein Sci. 13 (2004) 1466–1475.
[4] R.R. Draheim, A.F. Bormans, R.Z. Lai, M.D. Manson, Tryptophan residues flanking the second transmembrane helix (TM2) set the signaling state of the Tar chemoreceptor, Biochemistry 44 (2005) 1268–1277.
[5] J.A. Killian, I. Salemink, M.R. de Planque, G. Lindblom, R.E. Koeppe II, D.V. Greathouse, Induction of nonbilayer structures in diacylphosphatidylcholine model membranes by transmembrane alpha-helical peptides: importance of hydrophobic mismatch and proposed role of tryptophans, Biochemistry 35 (1996) 1037–1045.
[6] M.R. de Planque, J.W. Boots, D.T. Rijkers, R.M. Liskamp, D.V. Greathouse, J.A. Killian, The effects of hydrophobic mismatch between phosphatidylcholine bilayers and transmembrane alpha-helical peptides depend on the nature of interfacially exposed aromatic and charged residues, Biochemistry 41 (2002) 8396–8404.
[7] I. Nilsson, A. Saaf, P. Whitley, G. Gafvelin, C. Waller, G. von Heijne, Proline-induced disruption of a transmembrane alpha-helix in its natural environment, J. Mol. Biol. 284 (1998) 1165–1175.
[8] P. Braun, G. von Heijne, The aromatic residues Trp and Phe have different effects on the positioning of a transmembrane helix in the microsomal membrane, Biochemistry 38 (1999) 9778–9782.
[9] N.J. Gleason, V.V. Vostrikov, D.V. Greathouse, C.V. Grant, S.J. Opella, R.E. Koeppe II, Tyrosine replacing tryptophan as an anchor in GWALP peptides, Biochemistry 51 (2012) 2044–2053.
[10] K.A. Sparks, N.J. Gleason, R. Gist, R. Langston, D.V. Greathouse, R.E. Koeppe II, Comparisons of interfacial Phe, Tyr, and Trp residues as determinants of orientation and dynamics for GWALP transmembrane peptides, Biochemistry 53 (2014) 3637–3645.
[11] J.J. Falke, A.H. Erbse, The piston rises again, Structure 17 (2009) 1149–1151.
[12] J.J. Falke, G.L. Hazelbauer, Transmembrane signaling in bacterial chemoreceptors, Trends Biochem. Sci. 26 (2001) 257–265.
[13] A.S. Miller, J.J. Falke, Side chains at the membrane–water interface modulate the signaling state of a transmembrane receptor, Biochemistry 43 (2004) 1763–1770.
[14] B. Isaac, G.J. Gallagher, Y.S. Balazs, L.K. Thompson, Site-directed rotational resonance solid-state NMR distance measurements probe structure and mechanism in the transmembrane domain of the serine bacterial chemoreceptor, Biochemistry 41 (2002) 3025–3036.
[15] M. Welch, K. Oosawa, S. Aizawa, M. Eisenbach, Phosphorylation-dependent binding of a signal molecule to the flagellar switch of bacteria, Proc. Natl. Acad. Sci. U. S. A. 90 (1993) 8787–8791.
[16] S. Ravid, P. Matsumura, M. Eisenbach, Restoration of flagellar clockwise rotation in bacterial envelopes by insertion of the chemotaxis protein CheY, Proc. Natl. Acad. Sci. U. S. A. 83 (1986) 7157–7161.
[17] J.F. Hess, K. Oosawa, N. Kaplan, M.I. Simon, Phosphorylation of three proteins in the signaling pathway of bacterial chemotaxis, Cell 53 (1988) 79–87.
[18] K.A. Borkovich, N. Kaplan, J.F. Hess, M.I. Simon, Transmembrane signal transduction in bacterial chemotaxis involves ligand-dependent activation of phosphate group transfer, Proc. Natl. Acad. Sci. U. S. A. 86 (1989) 1208–1212.
[19] H.U. Ferris, K. Zeth, M. Hulko, S. Dunin-Horkawicz, A.N. Lupas, Axial helix rotation as a mechanism for signal regulation inferred from the crystallographic analysis of the *E. coli* serine chemoreceptor, J. Struct. Biol. 186 (2014) 349–356.
[20] H.U. Ferris, S. Dunin-Horkawicz, L.G. Mondejar, M. Hulko, K. Hantke, J. Martin, J.E. Schultz, K. Zeth, A.N. Lupas, M. Coles, The mechanisms of HAMP-mediated signaling in transmembrane receptors, Structure 19 (2011) 378–385.
[21] H.U. Ferris, S. Dunin-Horkawicz, N. Hornig, M. Hulko, J. Martin, J.E. Schultz, K. Zeth, A.N. Lupas, M. Coles, Mechanism of regulation of receptor histidine kinases, Structure 20 (2012) 56–66.
[22] M. Hulko, F. Berndt, M. Gruber, J.U. Linder, V. Truffault, A. Schultz, J. Martin, J.E. Schultz, A.N. Lupas, M. Coles, The HAMP domain structure implies helix rotation in transmembrane signaling, Cell 126 (2006) 929–940.
[23] M. Inouye, Signaling by transmembrane proteins shifts gears, Cell 126 (2006) 829–831.
[24] J.E. Schultz, J. Natarajan, Regulated unfolding: a basic principle of intraprotein signaling in modular proteins, Trends Biochem. Sci. 38 (2013) 538–545.
[25] J.J. Falke, Piston versus scissors: chemotaxis receptors versus sensor His-kinase receptors in two-component signaling pathways, Structure 22 (2014) 1219–1220.
[26] K.S. Molnar, M. Bonomi, R. Pellarin, G.D. Clinthorne, G. Gonzalez, S.D. Goldberg, M. Goulian, A. Sali, W.F. DeGrado, Cys-scanning disulfide crosslinking and bayesian modeling probe the transmembrane signaling mechanism of the histidine kinase, PhoQ, Structure 22 (2014) 1239–1251.
[27] B.A. Hall, J.P. Armitage, M.S.P. Sansom, Transmembrane helix dynamics of bacterial chemoreceptors supports a piston model of signalling, PLoS Comput. Biol. 7 (2011) e1002204.
[28] T. Hessa, N.M. Meindl-Beinker, A. Bernsel, H. Kim, Y. Sato, M. Lerch-Bader, I. Nilsson, S.H. White, G. von Heijne, Molecular code for transmembrane-helix recognition by the Sec61 translocon, Nature 450 (2007) 1026–1030.
[29] T.K. Nyholm, S. Ozdirekcan, J.A. Killian, How protein transmembrane segments sense the lipid environment, Biochemistry 46 (2007) 1457–1465.
[30] M. Kozak, Initiation of translation in prokaryotes and eukaryotes, Gene 234 (1999) 187–208.
[31] A. Saaf, E. Wallin, G. von Heijne, Stop-transfer function of pseudo-random amino acid segments during translocation across prokaryotic and eukaryotic membranes, Eur. J. Biochem. 251 (1998) 821–829.
[32] W. Hsing, T.J. Silhavy, Function of conserved histidine-243 in phosphatase activity of EnvZ, the sensor for porin osmoregulation in *Escherichia coli*, J. Bacteriol. 179 (1997) 3729–3735.
[33] T. Hessa, H. Kim, K. Bihlmaier, C. Lundin, J. Boekel, H. Andersson, I. Nilsson, S.H. White, G. von Heijne, Recognition of transmembrane helices by the endoplasmic reticulum translocon, Nature 433 (2005) 377–381.
[34] C. Lundin, H. Kim, I. Nilsson, S.H. White, G. von Heijne, Molecular code for protein insertion in the endoplasmic reticulum membrane is similar for N(in)-C(out) and N(out)-C(in) transmembrane helices, Proc. Natl. Acad. Sci. U. S. A. 105 (2008) 15702–15707.
[35] A. Stefansson, A. Armulik, I. Nilsson, G. von Heijne, S. Johansson, Determination of N- and C-terminal borders of the transmembrane domain of integrin subunits, J. Biol. Chem. 279 (2004) 21200–21205.
[36] A. Armulik, I. Nilsson, G. von Heijne, S. Johansson, Determination of the border between the transmembrane and cytoplasmic domains of human integrin subunits, J. Biol. Chem. 274 (1999) 37030–37034.
[37] T.L. Lau, V. Dua, T.S. Ulmer, Structure of the integrin alphaIIb transmembrane segment, J. Biol. Chem. 283 (2008) 16162–16168.
[38] T.L. Lau, A.W. Partridge, M.H. Ginsberg, T.S. Ulmer, Structure of the integrin beta3 transmembrane segment in phospholipid bicelles and detergent micelles, Biochemistry 47 (2008) 4008–4016.
[39] T.L. Lau, C. Kim, M.H. Ginsberg, T.S. Ulmer, The structure of the integrin alphaIIbbeta3 transmembrane complex explains integrin transmembrane signalling, EMBO J. 28 (2009) 1351–1361.
[40] D. Stopar, R.B. Spruijt, C.J. Wolfs, M.A. Hemminga, Local dynamics of the M13 major coat protein in different membrane-mimicking systems, Biochemistry 35 (1996) 15467–15473.
[41] M. Monne, I. Nilsson, M. Johansson, N. Elmhed, G. von Heijne, Positively and negatively charged residues have different effects on the position in the membrane of a model transmembrane helix, J. Mol. Biol. 284 (1998) 1177–1183.
[42] J.S. Parkinson, Signaling mechanisms of HAMP domains in chemoreceptors and sensor kinases, Annu. Rev. Microbiol. 64 (2010) 101–122.
[43] Q. Zhou, P. Ames, J.S. Parkinson, Biphasic control logic of HAMP domain signaling in the *Escherichia coli* serine chemoreceptor, Mol. Microbiol. 80 (2011) 596–611.
[44] S. Kitanovic, P. Ames, J.S. Parkinson, Mutational analysis of the control cable that mediates transmembrane signaling in the *Escherichia coli* serine chemoreceptor, J. Bacteriol. 193 (2011) 5062–5072.
[45] H. Park, W. Im, C. Seok, Transmembrane signaling of chemotaxis receptor tar: insights from molecular dynamics simulation studies, Biophys. J. 100 (2011) 2955–2963.
[46] G.A. Wright, R.L. Crowder, R.R. Draheim, M.D. Manson, Mutational analysis of the transmembrane helix 2-HAMP domain connection in the *Escherichia coli* aspartate chemoreceptor tar, J. Bacteriol. 193 (2011) 82–90.
[47] C.A. Adase, R.R. Draheim, G. Rueda, R. Desai, M.D. Manson, Residues at the cytoplasmic end of transmembrane helix 2 determine the signal output of the TarEc chemoreceptor, Biochemistry 52 (2013) 2729–2738.
[48] C.A. Adase, R.R. Draheim, M.D. Manson, The residue composition of the aromatic anchor of the second transmembrane helix determines the signaling properties of the aspartate/maltose chemoreceptor Tar of *Escherichia coli*, Biochemistry 51 (2012) 1925–1932.
[49] Q. Zhou, P. Ames, J.S. Parkinson, Mutational analyses of HAMP helices suggest a dynamic bundle model of input–output signalling in chemoreceptors, Mol. Microbiol. 73 (2009) 801–814.
[50] N. Sal-Man, D. Gerber, I. Bloch, Y. Shai, Specificity in transmembrane helix–helix interactions mediated by aromatic residues, J. Biol. Chem. 282 (2007) 19753–19761.
[51] S.D. Goldberg, G.D. Clinthorne, M. Goulian, W.F. DeGrado, Transmembrane polar interactions are required for signaling in the *Escherichia coli* sensor kinase PhoQ, Proc. Natl. Acad. Sci. U. S. A. 107 (2010) 8141–8146.
[52] S. Unnerstale, L. Maler, R.R. Draheim, Structural characterization of AS1-membrane interactions from a subset of HAMP domains, Biochim. Biophys. Acta 1808 (2011) 2403–2412.
[53] M. Kollmann, L. Lovdok, K. Bartholome, J. Timmer, V. Sourjik, Design principles of a bacterial signalling network, Nature 438 (2005) 504–507.
[54] P. Cluzel, M. Surette, S. Leibler, An ultrasensitive bacterial motor revealed by monitoring signaling proteins in single cells, Science 287 (2000) 1652–1655.